Article

Metal-Assisted Oxygen Atom Addition to an Fe(III)-Thiolate.

Gloria Villar-Acevedo, Priscilla Lugo-Mas, Maike Blakely, Abbie S. Ganas, Erin M. Hanada, Werner Kaminsky, and Julie A. Kovacs

J. Am. Chem. Soc., **Just Accepted Manuscript** • DOI: 10.1021/jacs.6b03512 • Publication Date (Web): 06 Dec 2016

Metal-Assisted Oxygen Atom Addition to an Fe(III)-Thiolate.

Gloria Villar-Acevedo, Priscilla Lugo-Mas, Maike N. Blakely, Abbie S. Ganas, Erin M. Hanada, [§]Werner Kaminsky and *Julie A. Kovacs

The Department of Chemistry, University of Washington, Box 351700

Seattle, WA 98195-1700

Received date: (to be automatically inserted once manuscript is accepted)

Title running head: Fe(III)-(RS-O) via Addition of PhIO to Fe(III)-SR

Corresponding author: J. Kovacs, tel. (206)543-0713, FAX (206)685-8665, kovacs@chem.washington.edu

[§] UW staff crystallographer

Abstract.

Cysteinate oxygenation is intimately tied to the function of both cysteinate dioxygenases (CDO) and nitrile hydratases (NHases), and yet the mechanisms by which sulfurs are oxidized by these enzymes are unknown, in part because intermediates have yet to be observed. Herein, we report a five-coordinate bis-thiolate ligated Fe(III) complex, $[Fe^{III}(S_2{}^{Me2}N_3(Pr,Pr))]^+$ (**2**), that reacts with oxo atom donors (PhIO and H_2O_2) to afford a rare example of a singly oxygenated sulfenate, $[Fe^{III}(\eta^2\text{-}S^{Me2}O)(S^{Me2})N_3(Pr,Pr)]^+$ (**5**), resembling both a proposed intermediate in the CDO catalytic cycle, as well as the essential NHase $Fe\text{–}S(O)^{Cys114}$ proposed to be intimately involved in its mechanism. Comparison of the reactivity of **2** with that of a more electron-rich, crystallographically characterized derivative, $[Fe^{III}S_2{}^{Me2}N^{Me}N_2{}^{amide}(Pr,Pr)]^{1-}$ (**8**), shows that oxo atom donor reactivity correlates with the metal ion's ability to bind exogenous ligands. Direct attack at the thiolate sulfurs of **2** is ruled out by DFT calculations, which show that the average spin-density on the thiolate sulfurs is approximately the same for **2** and **8**, and Mulliken charges on the sulfurs of **8** are roughly twice that of cationic **2,** implying that **8** should be more susceptible to sulfur oxidation. In contrast to imine-ligated **2**, carboxamide-ligated **8** is shown to be unreactive towards oxo atom donors. Azide (N_3^-) is shown to inhibit sulfur oxidation with **2**, and a green intermediate is observed to form, which then slowly converts, with clear isobestic points, to sulfenate-ligated **5**. This suggests that the mechanism of sulfur oxidation involves initial coordination of the oxo atom donor to the metal ion. Whether the green intermediate is an oxo atom donor adduct, Fe-O=I-Ph, or an Fe(V)=O remains to be determined.

Introduction.

Cysteinate dioxygenases (CDO) are non-heme Fe-enzymes that catalyze the O_2-promoted oxygenation of cysteinate ($^{Cys}S^-$) to cysteine sulfinic acid ($^{Cys}SO_2^-$).[1-8] A singly oxygenated cysteine sulfenate ($^{Cys}SO^-$) is proposed to be involved as an intermediate. High levels of cysteine can cause neurological disorders such as Parkinson's, Alzheimer's, and rheumatoid arthritis,[5,9] and thus having a mechanism for its degradation is important to human health. The CDO enzyme has also been shown to suppress tumor growth by combatting its defense against reactive oxygen species.[10] An epigenetic event can turn off CDO tumor suppression,[11] however, via methylation of the gene responsible for the biosynthesis of CDO. Methylated CDO genes are found in ~60% of breast cancers, and correlates with the progression of the disease and outcome.[12] The CDO mechanism (Figure 1) is proposed to involve cysteinate binding to the metal ion, followed by O_2 binding, *cis* to the $^{cys}S^-$, to afford an Fe^{III}-$O_2^{\bullet-}$ intermediate (**A**). The superoxo radical is then proposed to couple with the Fe^{II}-$^{cys}S\bullet \leftrightarrow$ Fe^{III}-$^{cys}S^-$ sulfur to afford a four membered ring structure RS-Fe^{II}-O-O (**B**). This step is unprecedented, in part because there are very few reported Fe^{III}-$O_2^{\bullet-}$,[8,13,14] but more importantly, because none have RS^- ligands in the coordination sphere. Upon heterolytic cleavage of the O-O bond, a high-valent iron oxo intermediate with a singly oxygenated sulfenate (RSO)Fe^{IV}=O (**C**) is proposed to form, which undergoes cis-migration to afford the final doubly oxygenated cysteine sulfinate.[1,5] Although theoretical calculations have indicated that the direct involvement

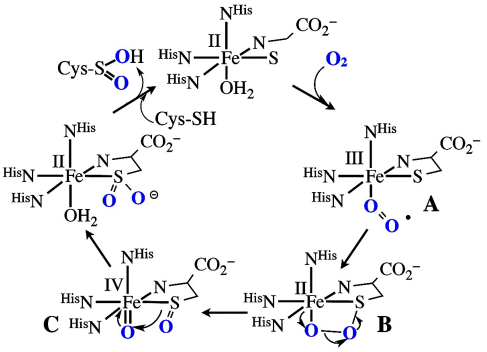

Figure 1.

of the metal ion of CDO provides a lower energy pathway to sulfur oxygenation,[1,5] this has not been experimentally proven. Intermediates **A**-**C** (Figure 1) have yet to be observed. The lack of spectroscopic data for any of the proposed CDO intermediates has made it impossible to calibrate theoretical calculations.[5]

Dioxygen has been shown to react with small molecule iron thiolate (RS^-) complexes to afford doubly or triply oxygenated thiolates.[15-20] For example, cysteinate-ligated $TpFe^{II}S^{cys}$ reacts with O_2 to afford $^{cys}SO_2^-$ (the product of CDO[5]), however, no intermediates were observed.[21] Iron complexes containing a non-tethered, monodentate RS-ligand *trans* to the O_2 binding site have been shown to react with O_2 to afford a Fe^{IV}=O + RSSR,[3,22] in contrast to *cis* thiolate-ligated complexes, which have been shown to react with O_2 to afford doubly (RSO_2-Fe), or triply (RSO_3-Fe) oxygenated derivatives.[1-4,22,23] Singly oxygenated RSO-Fe sulfenate intermediates are not observed in these cases. Whether these reactions are metal-mediated, or involve direct attack of O_2 at sulfur, has not been determined, although the orientation-dependence would suggest that they are. The mechanism of O_2-induced oxygenation of Ni-thiolate complexes, on the other hand, has been shown to involve direct attack by O_2 at the thiolate sulfurs.[24]

Oxygenated cysteinates have been shown to play a growing number of diverse roles in cellular processes, including T-cell activation, redox signaling in mammalian cells,[25] signal transduction, oxygen metabolism, oxidative stress response, and transcriptional regulation.[25,26] They are also required for enzyme activity in some cases (e.g, NHase[27-31], NADH peroxidase,[32] and peroxiredoxins[33]).

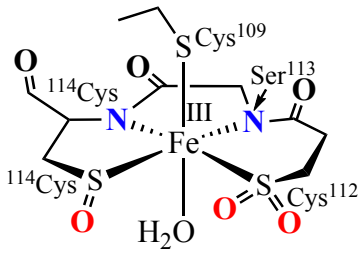

Scheme 1.

Nitrile hydratases (NHases) are a class of thiolate-ligated non-heme iron enzymes for which cysteinate oxygenation is intimately tied to function. These enzymes, which catalyze the enantioselective hydrolysis of nitriles to amides,[34-38] contain an Fe(III) (or Co(III)) active site ligated by three cysteinates, two of which are post-translationally modified (Scheme 1), one to a sulfenic acid (^{114}Cys–S–OH),[31,39,40] and the other to a sulfinate (^{112}Cys–SO_2^-).[41] Sulfur K-edge XAS studies have shown that the NHase sulfenic acid residue is protonated,[39] whereas the sulfinate (RSO_2^-) remains unprotonated.[39] The enzyme becomes inactive when a second oxygen atom is added to the sulfenic acid, ^{114}Cys–S–OH, implying that it plays a specific role in catalysis.[42] This is supported by time-resolved crystallography,[43] and crystallographic characterization of ^{114}Cys–S-bound inhibitors.[31] Coupled with theoretical calculations,[27] this experimental data provides evidence that *the sulfenate oxygen is intimately involved in the NHase mechanism*. The mechanism by which post-translationally modified NHase sulfenate and sulfinate oxygens are inserted has been proposed to involve O_2–induced formation of a thiolate-ligated high-valent oxo intermediate.[22,29] There is no experimental data available to verify this possibility, however.

Singly oxygenated sulfenates are difficult to trap,[26,44-47] even when they are coordinated to a metal ion (i.e., M-S(R)O$^-$).[24,48,49] There are significantly more examples of doubly oxygenated, metal-sulfinate (RSO_2^-) complexes.[15-20] Examples of singly oxygenated RS=O or RS-OH compounds include, $[Co^{III}(\eta^2\text{-SO})(SO_2)N_3(Pr,Pr)]^+$ (Scheme 2),[49] $[Fe^{III}(ADIT)(ADIT\text{-}O)]^+$ (**1**),[48] and

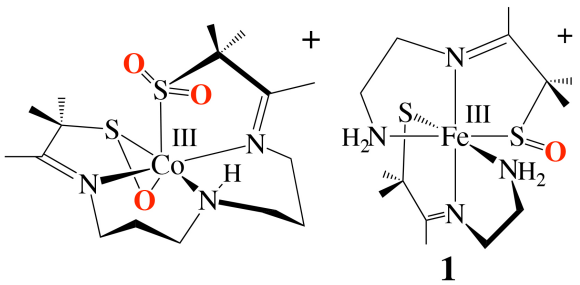

Scheme 2

$[Fe^{III}(ADIT)(ADIT\text{-}OH)]^{2+}$.[48]

In order to understand how thiolates promote O_2-activation,[50-52] tune reactivity and the electronic, magnetic, and reactivity properties of peroxo, oxo, and hydroxo intermediates, we have been exploring the reactivity of coordinatively unsaturated thiolate-ligated Fe (and Mn) complexes with dioxygen and its reduced derivatives.[51,53-59] Although an open coordination site is required for O_2 binding, thiolates are known to intercept open coordination sites by forming intermolecular M-SR-M bridges resulting in oligomerization. Despite this, we,[17,51,54,59-67] and others,[2,3,16,18,68-70] have synthesized a variety of coordinatively unsaturated mononuclear thiolate-ligated iron complexes that are capable of binding small molecules. For example, thiolate ligated $[Fe^{II}(N_4S^{Me2}(tren))]^+$,[54,71] and bis-thiolate ligated $[Fe^{III}(S_2{}^{Me2}N_3(Pr,Pr))]$ (**2**)[63] (Scheme 3), are five-coordinate, and contain flexible ligands capable of accommodating a sixth ligand,[62,63,72] as well as a variety of metal ions, in multiple oxidation states.[59,60,62,63,72-74] Both ligands constrain the geometry so that added "substrates" are forced to bind *cis* to a thiolate (e.g., structures **3** and **4**, Scheme 4).[64,65,75,76] For example, superoxide (O_2^-) reacts with reduced $[Fe^{II}(N_4S^{Me2}(tren))]^+$ at low temperatures in the presence of a proton donor[59,75,77] to afford a metastable, low-spin (S= ½; $g_\perp$ = 2.14; $g_{||}$ = 1.97) hydroperoxo intermediate $[Fe^{III}(N_4S^{Me2}(tren))(OOH)]^+$

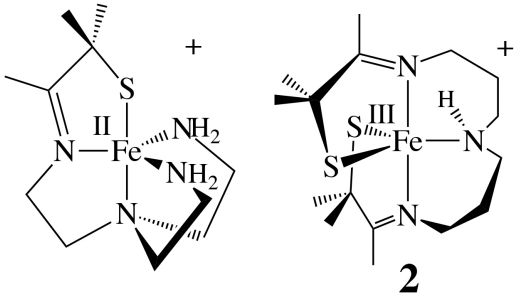

Scheme 3.

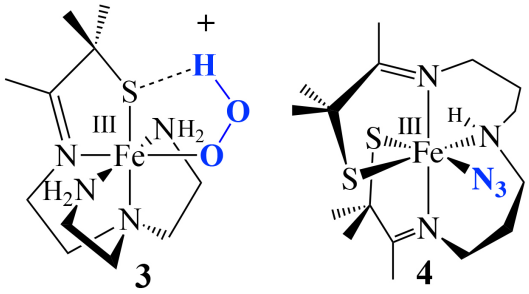

Scheme 4.

(**3**; Scheme 4; $\nu_{O\text{-}O}$= 784 cm^{-1}).[54] Bis-thiolate ligated **2** (Scheme 3) was shown to bind L= N_3^- (**4**) and NO *cis* to one of the thiolates, and *trans* to the other (Scheme 4).[63,78] Despite the π-donor properties of RS^- ligands, the highly covalent Fe-S bonds of oxidized $[Fe^{III}(N_4S^{Me2}(tren))L]^+$ (L = MeCN, HOO^- (**3**)),[54,64,65] $[Fe^{III}(S_2{}^{Me2}N_3(Pr,Pr))]^+$ (**2**) and $[Fe^{III}(S_2{}^{Me2}N_3(Pr,Pr))(N_3)]$ (**4**)[63] were all shown to favor a low spin-state (S= ½), due to the nephalauxetic effect.[79] The *trans* thiolate of **4** was shown to labilize the azide,[63] thereby promoting reversible L-binding.[80] Herein we examine the reactivity of bis-thiolate ligated $[Fe^{III}(S_2{}^{Me2}N_3(Pr,Pr))]^+$ (**2**, Scheme 3) with oxo atom donors, in order to determine how the presence of both a *cis* and *trans* thiolate influences electronic structure and reactivity.

Experimental Section.

General Methods. All reactions were performed under an atmosphere of dinitrogen in a glove box, using standard Schlenk techniques, or using a custom–made solution cell equipped with a threaded glass connector sized to fit a dip probe. Reagents purchased from commercial vendors were of the highest purity available and used without further purification. Toluene, tetrahydrofuran (THF), diethyl ether (Et_2O), and acetonitrile (MeCN) were rigorously degassed and purified using solvent purification columns housed in a custom stainless steel cabinet, dispensed via a stainless steel Schlenk-line (GlassContour). Methanol (MeOH) and ethanol (EtOH) were distilled from magnesium methoxide or ethoxide and degassed prior to use. Methylene chloride (DCM) was distilled from CaH_2 and degassed prior to use. ^1H NMR spectra were recorded on Bruker AV 300 or Bruker AV 301 FT-NMR spectrometers and are referenced to an

external standard of TMS (paramagnetic compounds) or to residual protio-solvent (diamagnetic compounds). Chemical shifts are reported in ppm and coupling constants (*J*) are in Hz. EPR spectra were recorded on a Bruker EPX CW-EPR spectrometer operating at X-band frequency at 7 K. IR spectra were recorded on a Perkin-Elmer 1700 FT-IR spectrometer as KBr pellets. Cyclic voltammograms were recorded in MeCN (100 mM $Bu^n_4N(PF_6)$ solutions) on a PAR 273 potentiostat utilizing a glassy carbon working electrode, platinum auxiliary electrode, and an SCE reference electrode. Magnetic moments (solution state) were obtained using the Evans' method as modified for super-conducting solenoids.[81,82] Temperatures were obtained using Van Geet's method. [83] Solid state magnetic measurements were obtained with polycrystalline samples in gel-caps using a Quantum Design MPMS S5 SQUID magnetometer. Ambient temperature electronic absorption spectra were recorded on a Hewlett-Packard Model 8450 spectrometer, interfaced to an IBM PC. Low temperature electronic absorption spectra were recorded using a Varian Cary 50 spectrophotometer equipped with a fiber optic cable connected to a "dip" ATR probe (C-technologies), with a custom–built two-neck solution sample holder equipped with a threaded glass connector (sized to fit the dip probe). Elemental Analyses were performed by Galbraith Labs, Knoxville, TN and Atlantic Microlabs, Norcross, GA. Thiolate–ligated $[Fe^{III}(S_2{}^{Me2}N_3(Pr,Pr))](PF_6)$ (**2**) was synthesized as previously described.[63]

Synthesis of $[Fe^{III}(\eta^2\text{-}S^{Me2}O)(S^{Me2}N_3(Pr,Pr)](PF_6)$ (5) via the Addition of PhIO to 2. To a stirred solution of $[Fe^{III}(S_2{}^{Me2}N_3(Pr,Pr))](PF_6)$ (**2**) (275 mg, 0.52 mmol) in MeOH (20 mL) at – 35 °C was added dropwise a 2 mL MeOH solution containing 1.2 equiv of PhIO (137 mg, 0.62 mmol). The solution was allowed to stir for 1 h at –35 ˚C, and then

stored in the freezer overnight. After filtration, the volume was reduced to 3 mL, layered with 25 mL of Et_2O, and cooled to – 35 °C overnight to afford **5** (153 mg, 0.28 mmol, 54%) as a pink crystalline solid. Electronic absorption (CH_3CN): λ_{max} (**ε**) = 333(4410), 510(1540) nm; (MeOH): λ_{max} (**ε**) = 325(4870), 510(1700), 760(248) nm (Figure S-1). IR (KBr pellet) $\nu(cm^{-1})$: 1625 (C=N); 1024 (S-O). Reduction Potential (MeCN): $E^{p,c}$ = – 0.960 V (irrev.) vs SCE. Solution magnetic moment (310.2 K; MeOH) μ_{eff} = 1.99 BM. EPR (DCM/toluene glass (1:1), 7 K): g_1 = 2.17, g_2 = 2.11, g_3 = 1.98. ESI-MS calcd for $[FeC_{16}N_3S_2H_{31}O]^+$: 401.3; found: 401.2. Anal. calcd for $FeC_{16}H_{31}N_3OS_2PF_6$: C, 35.2; H, 5.7; N, 7.7. Found: C, 35.39; H, 5.57; N, 7.77.

Formation of $[Fe^{III}(\eta^2\text{-}S^{Me2}O)(S^{Me2}N_3(Pr,Pr)](PF_6)$ (5) via the Addition of Hydrogen Peroxide to 2. Oxidized **2** (5 mg, 0.01 mmol) was dissolved in 20 mL of MeOH and placed in a sealed UV-vis dip-probe cell under a N_2 atmosphere. To this, 1.0 equiv of H_2O_2 (1 µL of a 30 % aqueous solution, 0.01 mmol) was added at room temperature via syringe to afford a pink air stable compound (**λ_{max}**= 510(1540) nm; EIS-MS (M+1): 401). Complex **5** is stable both at room temperature and in air.

Synthesis of $(Et_4N)[Fe^{III}S_2{}^{Me2}N^{Me}N_2{}^{amide}(Pr,Pr)]$ (8). To a stirred solution of $(HS^{Me})_2(N^{Me})(HN^{amide})_2(Pr,Pr)$•HCl (**C**, see supplemental for synthesis) (100 mg, 0.26 mmol) in MeOH (5 mL) at -35 °C was added dropwise a pre-cooled (-35 °C) solution of $(Et_4N)[FeCl_4]$ (85 mg, 0.26 mmol) in MeOH (3 mL). A pre-cooled (-35 °C) solution of NaOMe (70 mg, 1.3 mmol) in MeOH (5 mL) was then added, and the resulting reaction mixture was allowed to stir overnight at ambient temperature. The intense olive green solution was filtered and concentrated to dryness. The solid was re-dissolved in MeCN

and filtered. The filtrate was concentrated to a minimum amount of MeCN (~2 mL), layered with 10 mL of Et_2O, and cooled to -35 °C overnight to afford **8** (110 mg, 0.21 mmol, 80%) as a dark green crystalline solid. Electronic absorption (CH_3CN): λ_{max} (ε) = 352(8210), 428(3590), 581(1280) nm; (MeOH): λ_{max} (ε) = 348(8150), 588(1210) nm; (H_2O): λ_{max} (ε) = 352(8060), 584(1530) nm. IR (KBr pellet) ν(cm^{-1}): 1564 (C=O). $E_{1/2}$ (MeCN) = -1.51 V vs SCE. Solution magnetic moment (298 K; MeOH) μ_{eff} = 3.75 BM. EPR (MeOH/EtOH glass (9:1), 9 K): g_1 = 4.72, g_2 = 2.82, g_3 = 1.92. ESI-MS calcd for $[FeC_{13}H_{21}N_2O_2S_3]^{1-}$: 389.4, found: 389.3. Anal. calcd for $FeC_{23}H_{47}N_4O_2S_2$: C, 52.0; H, 8.9; N, 10.5. Found: C, 52.3; H, 8.87; N, 10.49.

Formation of a Green Intermediate, via the Addition of IBX-ester to 2. A 0.238 mM solution of **2** was prepared in 5 mL of MeOH under an inert atmosphere in a drybox. The resulting solution was transferred *via* gas-tight syringe to a custom-made two-neck vial equipped with a septum cap and threaded dip-probe feed-through adaptor that had previously been purged with argon and contained a stir bar. This solution was cooled in an acetone/dry ice bath to -73 ˚C. To this, 10 eq. of IBX-ester (isopropyl 2-iodoxybenzoate) (50 µL of 238 mM solution of IBX-ester in MeOH) was added, resulting in the formation of a meta-stable green intermediate (λ_{max}= 675 nm).

Formation of a Green Intermediate, via the Addition of PhIO to 2. A 0.238 mM solution of **2** was prepared in 5 mL of MeOH or THF under an inert atmosphere in a drybox. The resulting solution was transferred *via* gas-tight syringe to a custom-made two-neck vial equipped with a septum cap and threaded dip-probe feed-through adaptor that had previously been purged with argon and contained a stir bar. This solution was

cooled in an acetone/dry ice bath to -73 ˚C. To this, 1-4 eq. of PhIO (50-200 µL of 23.8 mM solution in MeOH) was added, resulting in the formation of a meta-stable intermediate (λ_{max}= 675 nm).

DFT Calculations. All geometry optimizations were performed utilizing the ORCA v.3.0 quantum chemistry package[84] and originated from X-ray crystallographic coordinates. A BP86 functional,[85,86] with the resolution of identity approximation (RI),[87] dispersion correction (D3BJ),[88] and zeroth-order regular approximation for relativistic effects (ZORA),[89] was employed, using a dense integration grid (Grid4), def2-TZVP basis set,[90] and def2-TZVP/J auxiliary basis set. In addition, the conductor-like screening model (COSMO) using acetonitrile (ε =37.5) as the solvent,[91] was employed. All optimized geometries were visualized using Avogadro.

X-ray Crystallographic Structure Determination. A red crystal plate 0.24 x 0.24 x 0.05 mm of **5** was mounted on a glass capillary with oil. Data was collected at -143 °C. The crystal-to-detector distance was set to 30 mm and exposure time was 30 seconds per degree for all data sets with a scan width of 1.4^{o}. The data collection was 89.1% complete to 28.34^{o} and 96.1% complete to 25^{o} in $\boldsymbol{\theta}$. A total of 63733 partial and complete reflections were collected covering the indices, h = -16 to 16, k = -18 to 20, l = -19 to 19. 5215 reflections were symmetry independent and the R_{int} = 0.0698 indicated that the data was of average quality (0.07). Indexing and unit cell refinements indicated a monoclinic P lattice in the space group P 21/c (No.14).

A black crystal prism size 0.48 x 0.44 x 0.36 mm of **8** was mounted on a glass capillary with oil. Data was collected at -143 °C. The crystal-to-detector distance was

set to 40 mm and exposure time was 20 seconds per degree for all sets with a scan width of 1.5°. The data collection was 94.5% complete to 28.63° and 99.8% complete to 25° in θ. A total of 41494 partial and complete reflections were collected covering the indices, h = -23 to 23, k = -11 to 11, l = -23 to 23. 6353 reflections were symmetry independent and the R_{int} = 0.063 indicated that the data was of average quality (0.07). Indexing and unit cell refinement indicated an orthorhombic P lattice in the space group P n a 2_1 (No.33).

The data for both **5** and **8** was integrated and scaled using Denzo-hkl-SCALEPACK, and an absorption correction was performed using SORTAV. Scattering factors were obtained from Waasmair and Kirfel.[92] Solution by direct methods (SIR97) produced a complete heavy atom phasing model consistent with the proposed structures. All non-hydrogen atoms were refined anisotropically by full-matrix least-squares methods, while all hydrogen atoms were then located using a riding model. Crystal data for **5** and **8** is presented in Table 1 (below). Selected bond distances and angles are assembled in Table 2.

Table 1. Crystal data for $[Fe^{III}(\eta^2\text{-}S^{Me2}O)(S^{Me2}N_3(Pr,Pr)](PF_6)$ (**5**), and $(Et_4N)[Fe^{III}S_2{}^{Me2}N^{Me}N_2{}^{amide}(Pr,Pr)]$ (**8**).

	5	**8**
formula	$C_{16}H_{31}F_6FeN_3OPS_2$	$C_{23}H_{47}FeN_4O_2S_2$
MW (g/mol)	546.38	531.62
temp (K)	130(2)	130(2)
unit cell[a]	Monoclinic	Orthorhombic
space group	P 21/c	P n a 21
a (Å)	12.3550(5)	17.9580(3)
b (Å)	15.3070(8)	8.5610(6)
c (Å)	14.8020(7)	18.1560(7)
α (°)	90	90
β (°)	123.147(3)	90
γ (°)	90	90
V (Å^3)	2343.79(19)	2791.3(2)
Z	4	4
σ_{calc} (mg/m^3)	1.548	1.265
R[b]	0.0721	0.0477
R_w	0.2040	0.1219
GOF	1.001	0.940

[a] In all cases: Mo Kα(λ = 0.71070 Å) radiation.[b] $R = \Sigma||F_o| - |F_c||/\Sigma|F_o|$; $R_w = [\Sigma w(|F_o| - |F_c|)^2/\Sigma wF_o{}^2]^{1/2}$, where $w^{-1} = [\sigma^2_{count} + (0.05F^2)^2]/4F^2$.

Results and Discussion.

Addition of 1.2 equiv of PhIO to five-coordinate $[Fe^{III}(S_2{}^{Me2}N_3(Pr,Pr))]^+$ (**2**)[63] at ambient temperatures induces a color change from orange to magenta, and causes the S→Fe CT band in the electronic absorption spectrum, at 415(4200) nm, to disappear, and a new band to grow in at 510(1540) nm (Figure 2). A red-shifted absorption band would be consistent with an increase in metal ion Lewis acidity, as a consequence of oxo atom addition. The ESI mass spec of this magenta species, **5**, shows a peak at *m/z* = 401 corresponding to the parent ion M + 16 (Figure S-2), consistent with the addition of a single oxygen atom. Addition of one equiv of H_2O_2 (aq) to **2** in MeOH (Figure S-3) affords an identical magenta-colored species (**5**, λ_{max}= 510(1540) nm), with an identical ESI-MS indicative of the addition of a single oxygen atom. Single oxo atom addition to **2** would be consistent with the formation of either a high-valent iron oxo, or an iron-sulfenate (FeS(R)–O^-) species. The low temperature (7 K), perpendicular-mode EPR spectrum of **5** (Figure 3) reproducibly

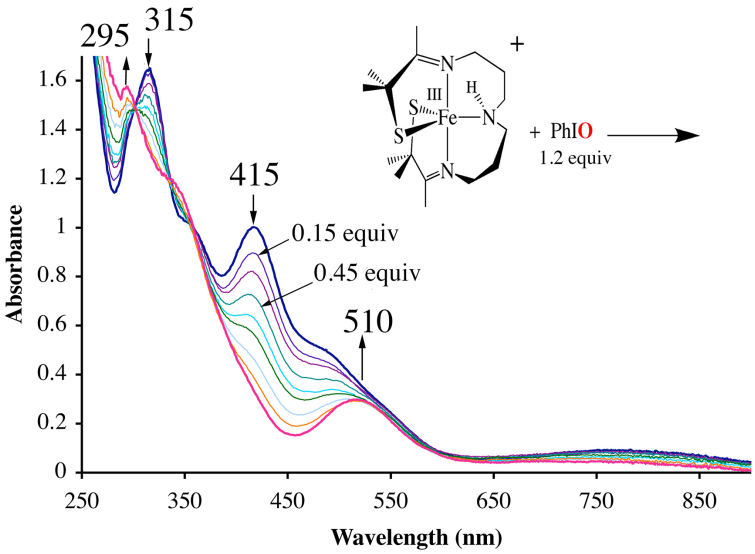

Figure 2. Using electronic absorption spectroscopy to monitor the reaction between $[Fe^{III}(S_2{}^{Me2}N_3(Pr,Pr))]^+$ (**2**) and 1.2 equiv of PhIO, added in 0.15 equiv aliquots, in MeOH at 298 K.

displays an intense rhombic signal with *g*–values of 2.16, 2.10 and 1.97 indicative of an S= ½ ground-state. The precursor to **5**, $[Fe^{III}(S_2{}^{Me2}N_3(Pr,Pr))]^+$ (**2**), is also low-spin S= ½, but has distinctly different g-values (*g* = 2.20, 2.15, 2.00).[63] The ambient temperature, MeOH solution magnetic moment of **5** (μ_{eff} = 1.99 BM), is also consistent with an S= ½ spin- state, and indicates that there are no thermally accessible higher spin-states in the range 7-300 K. In contrast, **2** has an ambient temperature magnetic moment of μ_{eff} = 3.5 BM reflecting the thermal accessibility of an S=3/2 excited state.[63] The S= ½ ground state of **5** would be consistent with either an Fe(V)[93-96] or an Fe(III) oxidation state,[48,54,59-61,63,66,79,97] but inconsistent with an even-spin, S= 1 or S= 2 system, thereby ruling out an Fe(IV)=O.

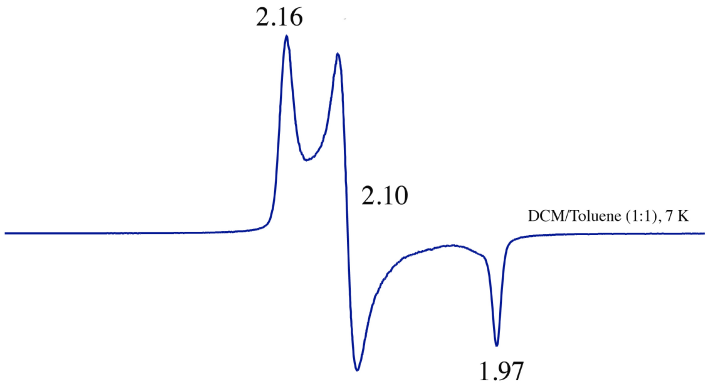

Figure 3. Low temperature (7 K) X-band EPR spectrum of **5** in CH_2Cl_2/Toluene (1:1) glass.

The redox properties of the **5** also differ from those of **2**. Whereas five-coordinate **2** is reversibly reduced at a potential of $E_{1/2}$= –425 mV vs SCE (Figure 4), **5** is irreversibly reduced at a significantly more negative potential (E_{pc}= –958 mV, E_{pa}= -690 mV vs SCE; Figure S-4). The latter is quasi-reversible. Oxygen atom addition therefore increases the stability of the Fe^{+3} oxidation state. Oxygenation at sulfur would be

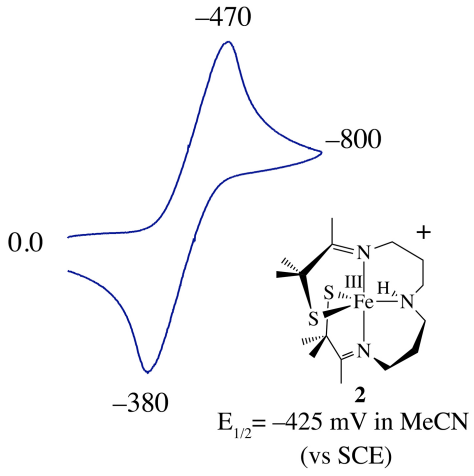

Figure 4. Cyclic voltammogram of five-coordinate $[Fe^{III}(S_2{}^{Me2}N_3(Pr,Pr))]^+$ (**2**) in MeCN at 298 K (0.1 M $(Bu_4N)PF_6$, glassy carbon electrode, 150 mV/sec scan rate). Peak potentials versus SCE indicated.

expected to shift the potential in the opposite direction, given that it would decrease the electron donating properties of the sulfur, unless, of course, the unmodified thiolate overcompensates for the increase in Lewis acidity by forming a more covalent unmodified Fe-SR bond.[48] If the latter were the case, then the S→Fe CT band should blue shift,[48] as opposed to red-shift as shown in Figure 2. On the other hand, ferric ions are more stable in a six-coordinate environment, relative to a five-coordinate environment, perhaps suggesting that oxo atom addition involves the metal ion.

Iodosyl benzene (PhIO) typically promotes 2-electron chemistry, and has been shown to convert Fe(II) compounds to Fe(IV)=O compounds.[98-101] There are fewer examples of Fe(III) compounds that are reactive towards oxo atom donors, such as PhIO (Figure 2).[102-104] One example of the latter involves the addition of PhIO to cytochrome P450 in its Fe(III) resting state, to afford (por/^{cys}S)Fe(V)=O (cmpd I).[105] The oxidizing equivalents of P450 cmpd I have been shown to be delocalized over both the redox active porphyrin (por) and redox active thiolate ligands.[106-111] Hydrogen peroxide (H_2O_2) has also been shown to convert Fe(III) compounds to Fe(V)=O species,[112,113] or its redox equivalent.[107,109,111] In contrast to Fe(IV)=O compounds,[52,98,114-123] however, very few synthetic non-heme Fe(V)=O species have been observed.[93,95,96,104,113,124] The most thoroughly characterized example, $[Fe(V)(TAML)(O)]^{-}$, incorporates an electron donating tetra-anionic carboxamide ligand (*vide infra*), $TAML^{4-}$.[93,95,104,125,126]

The IR spectrum of **5** contains a stretch at ν= 1024 cm^{-1} (Figure S-5) that is absent in the IR spectrum of **2**. This stretching frequency would be extremely high for an Fe(V)=O ($\nu_{Fe=O}$ = 798-828 cm^{-1})[96,127] and is somewhat above the usual range ($\nu_{S=O}$ = 970-900 cm^{-1})[24,35,46,128-130] for a metal-sulfenate complex. Sulfenate $\nu_{S=O}$ stretches have,

however, previously been shown to shift out of the usual range if the RS=O is η^2–coordinated to a metal ion.[49,131] For example, sulfenate/sufinate-ligated $[Co^{III}(\eta^2\text{-}SO)(SO_2)N_3(Pr,Pr)]^+$ (Scheme 2) has a sulfenate $\nu_{S=O}$ stretch at 1066 cm^{-1}.[49]

X-ray Structure of $[Fe^{III}(\eta^2\text{-}S^{Me2}O)(S^{Me2})N_3(Pr,Pr)]PF_6$ (5). The identity of the product, **5**, formed in the reaction between **2** and PhI, (or H_2O_2), was ultimately determined by X-ray crystallography. Single crystals of **5** were grown at -30 ˚C by layering Et_2O onto a MeCN solution. As shown in the ORTEP diagram of Figure 5, the single oxygen atom O(1) adds ~*trans* (O(1)-Fe-S(2)= 152.3(2)˚) to one of the thiolate sulfurs (S(2)), and forms a bond to the cis-thiolate S(1), affording an η^2-coordinated sulfenate $[Fe^{III}(\eta^2\text{-}S^{Me2}O)(S^{Me2})N_3(Pr,Pr)]^+$ (**5**). A similar side-on sulfenate (η^2-RSO^-) binding-mode was observed previously in $[Co^{III}(\eta^2\text{-}SO)(SO_2)N_3(Pr,Pr)]^+$ (Scheme 2).[49] As mentioned earlier, singly oxygenated metal sulfenates (RSO^-) are rare[24,48,49] since they tend to be more reactive than their thiolate precursor.[26,46,47,49] There are significantly more examples of doubly oxygenated, structurally–rearranged oxygen–bound, metal-sulfinate (RSO_2^-) complexes.[16-20]

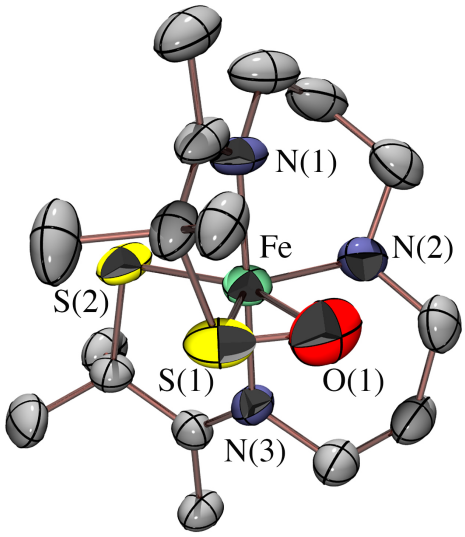

Figure 5. ORTEP of the cation of $[Fe^{III}(\eta^2\text{-}S^{Me2}O)(S^{Me2})N_3(Pr,Pr)](PF_6)$ (**5**) showing atom labeling scheme. All hydrogen atoms have been removed for clarity.

Comparison of structure **5** (Figure 4) with that of its $[Fe^{III}(S_2{}^{Me2}N_3(Pr,Pr))]^+$ (**2**) precursor (Table 2) shows that the singly oxygenated Fe-S(1) bond of **5** elongates only

slightly as a result of oxygen atom addition (from 2.133(2) Å in **2** to 2.142(2) Å in **5**). One would have expected a more dramatic change in bond length. The Fe-S(2) bond, on the other hand, decreases in length from 2.161(2) Å in **2** to 2.148(2) Å in **5**, indicating that the unmodified thiolate compensates for the shifting of electron density away from the metal ion towards the oxygen atom. This compensatory effect was observed previously with $[Fe^{III}(ADIT)(ADIT\text{-}O)]^{+}$ (**1**; Scheme 2).[48] The sulfenate S(1)-O(1) bond in **5** (1.447 Å; Table 2) is slightly shorter than the few known sulfenate complexes (range: 1.50–1.60 Å),[24,46,131] including that of $[Co^{III}((\eta^2\text{–}SO)(SO_2)N_3(Pr,Pr))]^{+}$ (Scheme 2) (S(1)-O(1), 1.548(3) Å).[49]

Table 2. Comparison of Selected bond distances (Å) and angles (deg) for Imine-Ligated $[Fe^{III}(S_2{}^{Me2}N_3(Pr,Pr))]^{+}$ (**2**),[63], its Singly Oxygenated Derivative $[Fe^{III}(\eta^2\text{-}S^{Me2}O)(S^{Me2}N_3(Pr,Pr)]^{+}$ (**5**), and Carboxamide-Ligated $[Fe^{III}S_2{}^{Me2}N^{Me}N_2{}^{amide}(Pr,Pr)]^{1-}$ (**8**).

	2	**5**	**8**
Fe-S(1)	2.133(2)	2.142(2)	2.231(1)
Fe-S(2)	2.161(2)	2.148(2)	2.210(1)
Fe-N(1)	1.967(4)	1.976(4)	1.934(3)
Fe-N(2)	2.049(4)	2.044(5)	2.212(3)
Fe-N(3)	1.954(4)	1.954(4)	1.924(3)
Fe-O(1)	N/A	2.115(4)	N/A
S(1)-O(1)	N/A	1.447(6)	N/A
N(1)-Fe-N(3)	178.1(2)	178.0(2)	177.8(1)
S(1)-Fe-S(2)	121.0(1)	112.62(8)	144.40(5)
S(1)-Fe-N(2)	132.3(1)	134.1(1)	107.14(9)
S(2)-Fe-N(2)	106.5(1)	113.2(2)	108.43(9)
S(1)-Fe-N(1)	86.7(1)	86.1(1)	85.37(9)
S(2)-Fe-N(1)	95.2(1)	91.9(1)	93.8(1)
S(1)-Fe-O(1)	N/A	39.7(2)	N/A**
O(1)-Fe-S(2)	N/A	152.3(2)	N/A**
O(1)-Fe-N(1)	N/A	87.6(2)	N/A**
O(1)-Fe-N(2)	N/A	94.3(2)	N/A**
O(1)-Fe-N(3)	N/A	94.4(2)	N/A**
τ	0.76	N/A	0.56

**In this structure the only oxygens are associated with the carboxamide, and are not coordinated to the metal.

Synthesis of a More Electron-Rich Derivative of 2. In order to provide an even more electron-rich environment, analogous to that of the $TAML^{4-}$ ligand shown previously to stabilize an Fe(V)=O,[93] we synthesized (Scheme S-1) the tetra-anionic carboxamide ligand $[(Pr,Pr)(N^{Me}N^{amide}{}_2S^{Me}{}_2)]^{4-}$ (Figure S-6–S-9), and its corresponding Fe-complex (Scheme 5). As mentioned earlier, the preferred 2e- chemistry of PhIO makes it conceivable that oxo atom addition to Fe(III)-**2** results in the formation of an unobserved metastable Fe(V)=O intermediate along the reaction pathway to **5**. The highly covalent Fe–S bonds would help to delocalize the oxidizing equivalents, thereby making the higher-valent state accessible. The placement of a nucleophilic thiolate *cis* to an electrophilic oxo would facilitate rapid intramolecular trapping of the oxo via the formation of an S-O bond. A similar reaction sequence was recently observed to convert a sulfur-bound substrate analogue of isopenicillin-N-synthase to an $Fe^{II}((\eta^2-SO)$,[132] and may be the mechanism by which the catalytically important sulfenate is inserted into the Fe-NHase active site.[27]

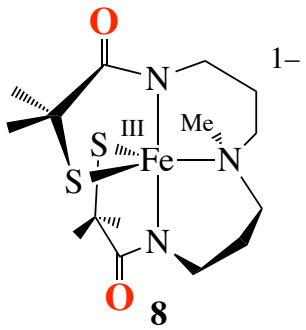

8

Scheme 5.

Bis-thiolate/carboxamide-ligated $[Fe^{III}S_2{}^{Me2}N^{Me}N_2{}^{amide}(Pr,Pr)]^{1-}$ (**8**) displays a $\nu_{C=O}$ stretch at 1564 cm^{-1} (Figure S-11), and parent ion peak in the negative-mode ESI-MS (Figure S-10). This would be consistent with the structure shown in Scheme 5, which incorporates anionic carboxamides in place of the neutral imines of **2**. X-ray quality crystals of $(Et_4N)[Fe^{III}S_2{}^{Me2}N^{Me}\ N_2{}^{amide}(Pr,Pr)]$ (**8**) were obtained via slow vapor diffusion of Et_2O into a MeCN solution at –35 ˚C. As shown in the ORTEP diagram of Figure 6, the Fe^{3+} ion of **8** maintains a five- coordinate structure, despite being crystallized from a

coordinating solvent (MeCN), and resides in a highly distorted N_3S_2 environment (τ = 0.56) halfway between trigonal bipyramidal and square pyramidal. The Fe^{3+} ion is ligated by two *cis*-thiolate sulfurs and a tertiary amine (N(2)) in the equatorial plane, and two *trans*- carboxamide nitrogens (N(1), N(3)) in apical positions. Key bond distances and angles are compared with those of its cationic imine analogue **2** in Table 2. The incorporation of anionic carboxamides in **8**, in place of the neutral imines of **2**, causes the mean Fe–S bond distance to significantly elongate (from 2.147 Å in **2** to 2.22 Å in **8**). A similar increase in Fe–S bond lengths (from 2.189 Å to 2.219 Å) is seen upon replacement of the neutral imines in $[Fe^{III}(tame\text{-}N_3)S_2^{Me2})]^+$, with anionic carboxamides in $[Fe^{III}((tame\text{–}N_2S)S_2^{Me2})]^{2-}$.[17] The S–Fe–S angle (144˚) in **8** is significantly wider than that of **2** (121˚), as well as imine-ligated $[Fe^{III}(S_2^{Me2}N_3(Et,Pr))]^+$ (105˚).[61]

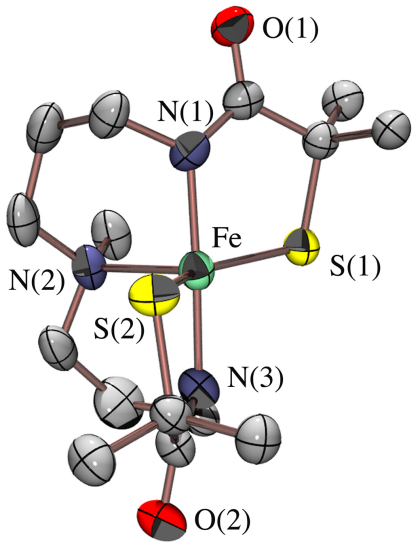

Figure 6. ORTEP of the anion of $(Et_4N)[Fe^{III}S_2^{Me2}N^{Me}N_2^{amide}(Pr,Pr)]$ (**8**) showing atom labeling scheme. All hydrogen atoms have been removed for clarity.

Carboxamide-ligated **8** is soluble

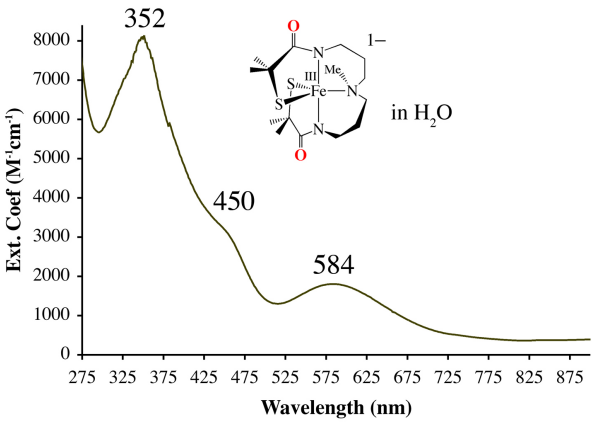

Figure 7. Electronic absorption spectrum of $(Et_4N)[Fe^{III}S_2^{Me2}N^{Me}N_2^{amide}(Pr,Pr)]$ (**8**) in H_2O at 298 K.

in a variety solvents,including H_2O, forms intense olive green-colored solutions, and displays a solvent-independent electronic absorption spectrum with bands at λ_{max}= 352(8060), 450(sh), and 584(1530) nm, indicating that solvents (MeCN, MeOH, H_2O (Figure 7)) do not coordinate to the metal ion. The redox potential of anionic **8** (–1.51V vs SCE; Figure 8) is shifted by over 1 V, relative to that of cationic imine-ligated **2** ($E_{1/2}$ = –425 mV vs SCE, Figure 4), demonstrating that carboxamide ligands provide significant stability to the Fe^{+3} oxidation state.[133]

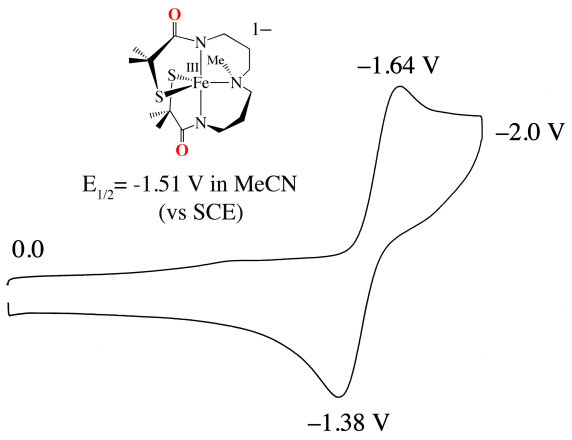

Figure 8. Cyclic voltammogram of $(Et_4N)[Fe^{III}S_2{}^{Me2}N^{Me}N_2{}^{amide}(Pr,Pr)]$ (**8**) in MeCN at 298 K (0.1 M $(Bu_4N)PF_6$, glassy carbon electrode, 150 mV/sec scan rate). Peak potentials versus SCE indicated.

As shown by fits to the inverse magnetic susceptibility ($1/\chi_m$) versus temperature plot of Figure 9, and low temperature (7 K) perpendicular-mode EPR (g =4.72, 2.82, 1.92; Figure S-12) bis-thiolate ligated **8** has an S= 3/2 ground state, and maintains this spin-state over a wide temperature range in the solid state and frozen solution. The ambient temperature MeCN solution magnetic moment of μ_{eff} = 3.75 μ_B indicates that **8** maintains this spin-state in solution. In contrast,

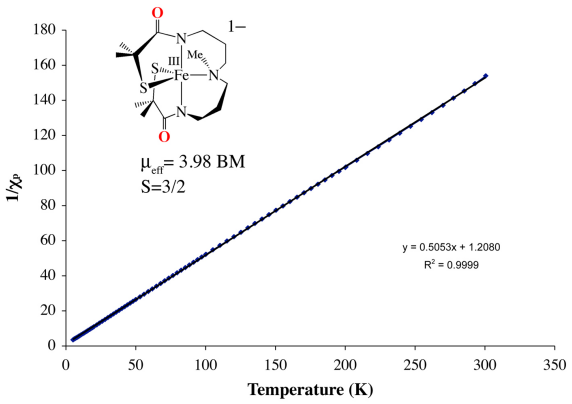

Figure 9. Inverse molar magnetic susceptibility $1/\chi_m$ *vs* temperature (T) plot for $(Et_4N)[Fe^{III}S_2{}^{Me2}N^{Me}N_2{}^{amide}(Pr,Pr)]$ (**8**) fit to an *S* = 3/2 spin-state.

imine-ligated **2** has an *S*=1/2 ground state, with a thermally accessible S= 3/2 state that is ~23% populated at ambient temperature, and 11% populated at T= -80 ˚C. Spin-states have been shown to influence reactivity in profound ways.[134,135]

Comparison of the Reactivity Properties of Carboxamide-Ligated 8 versus Imine-Ligated 2. In contrast to **2**, carboxamide-ligated **8** does not react with oxo atom donors PhIO or H_2O_2, under any conditions, even with a huge excess of oxidant, and over a wide temperature range (-78 ˚C – 25 ˚C). One would have anticipated that the thiolates of **8** would be more readily oxygenated, given the anionic molecular charge, and expected increase in electron density on the thiolate sulfurs. Given the similarity of its ligand environment to that of $[Fe(V)(TAML)(O)]^{-}$, one would have also anticipated that an Fe(V)=O might be stabilized, possibly to the point where it might be observable, prior to intramolecular trapping, and S-O bond formation. If, on the other hand, sulfur oxidation involves direct attack at the thiolate sulfurs, then one would also expect carboxamide-ligated **8** to be more reactive towards oxo atom donors than **2**, because the thiolate sulfurs should carry more negative charge. In order to determine whether the latter is indeed the case, and quantify this difference if it exists, we turned to theoretical calculations. Density functional theory (DFT) calculations were performed using the ORCA package, a BP86 functional and def2-TZVP basis set. For both **2** and **8**, metrical parameters of the DFT-optimized geometry are within ≤ 1.96 % of the crystallographically-determined bond lengths (Table S-1). Based on these calculations, the Mulliken charges on the sulfurs of anionic **8** (–0.484 for S(1), –0.488 for S(2)) were found to be roughly twice that of cationic **2** (–0.288 for S(1),–0.245 for S(2)). The longer

Fe–S bond distances in **8**, relative to **2**, would be consistent with this. The calculated average spin-density on the thiolate sulfurs is approximately the same for **2** (0.12) and **8** (0.15). Theoretical calculations therefore suggest that if oxo atom donors were to directly attack the thiolate sulfur in a 2e– process, then carboxamide-ligated **8** would be more reactive than imine-ligated **2**, when in fact the opposite is observed. If a 1e– radical process, involving direct attack at the sulfurs, were involved, then the two complexes **2** and **8** should be equally reactive. Oxo atom donor reactivity does, on the other hand, correlate with ligand binding properties. Despite its open coordination site, anionic **8** does not bind neutral (pyridine, MeCN) or anionic (N_3^-, CN^-) ligands, even when added in excess (>100 eq) at low temperatures (–40 ˚C to –78 ˚C), as determined using electronic absorption spectroscopy. This is likely due to the fact that a spin-state change would be required in order for 5-coordinate **8** to convert to a 6-coordinate structure. Whereas **8** is S=3/2, six-coordinate, thiolate-ligated ferric complexes are predominantly low-spin S=1/2.[39,59,79,97,136] As one would expect, calculated unpaired spin-density on the iron of **8** (2.59) is significantly larger than that of **2** (0.83), reflecting the S= ½ ground state of **2**. A Me-group on N(2) of **8**, in place of the N(2)-H proton of **2**, also likely inhibits ligands from binding to **8**, since it would sterically clash with S(1) when the S(1)-Fe-N(2) bond angle decreased as a consequence of a the concomitant geometry change (~trigonal bipyriamidal→ ~octahedral). Imine-ligated **2**, on the other hand, readily binds both N_3^- and NO to its open coordination site,[63,78] in addition to reacting with oxo atom donors.

Thus, both correlations between sulfur oxidation and the molecule's affinity for a sixth ligand and ability to undergo a geometry change, and theoretical calculations,

suggest that the mechanism of sulfur oxidation with **2** involves initial coordination of the oxo atom donor to the metal ion. Consistent with this, azide (N_3^-) is found to inhibit sulfur oxidation with **2**. If 1.2 equiv of N_3^- is added to **2** in THF at -73 ˚C, then the intense band 415(4200) nm characteristic of **2**, is replaced by a band at 708(1600) nm (Figure 10) characteristic of coordinatively saturated, azide-bound [$Fe^{III}(S_2{}^{Me2}N_3(Pr,Pr))(N_3)$] (**4**).[63] If, following the formation of azide-bound **4** in THF, 1.2 equiv of PhIO is added, no reaction is observed, even after prolonged reaction times (2 hr). If, under the same conditions (-73 ˚C in THF) 1.2 equiv of PhIO is added to **2**, in the absence of N_3^-, then a metastable intermediate that converts to singly oxygenated [$Fe^{III}(\eta^2\text{-}S^{Me2}O)(S^{Me2}N_3(Pr,Pr)]^+$ (**5**) (λ_{max}= 510(1540)) forms within minutes. Thus, azide inhibits sulfur oxidation with **2**, presumably by preventing the oxo atom donor from binding to the metal ion. Consistent with this, we observe an intermediate in the oxo atom donor reaction in the absence of azide.

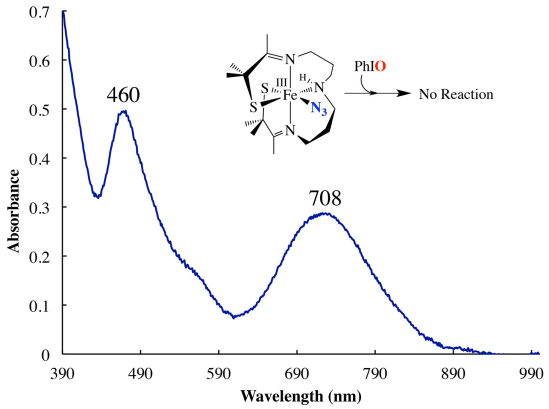

Figure 10. Monitoring the addition of iodosylbenzene (PhIO) to [$Fe^{III}(S_2{}^{Me2}N_3(Pr,Pr))N_3$] (**4**) in MeOH at -73 ˚C via electronic absorption spectroscopy showing that no reaction occurs.

Observation of an Intermediate in the Reaction Between Imine-Ligated 2 and Oxo Atom Donors PhIO and IBX-ester. If the reaction between 10 equiv of PhIO and five-coordinate **2** is monitored by electronic absorption spectroscopy at low temperatures (-73 ˚C) in MeOH, a green intermediate with a λ_{max}= 675 nm is observed (Figure S-13), which then slowly (t=360 min, [**2**]= 0.238 mM) converts to sulfenate-ligated **5** (Figure S-14). As shown in Figure 11, an ~identical intermediate (λ_{max}= 677 nm) is

formed when isopropyl 2-iodoxybenzoate (IBX-ester) is used in place of PhIO, however its rate of conversion to sulfenate-ligated **5** (36 min, [**2**]= 0.238 mM) is significantly faster. IBX-ester contains an $I^{V}(=O)_2$ moiety,[137] whereas PhIO contains an I^{III}=O moiety, providing a possible explanation for the differences in rates. The observation of intermediates in these reactions provides evidence that sulfur oxidation is assisted by the metal ion, and involves the initial binding of oxo-atom donors to Fe. Clear isobestic points visible during these reactions show that the new intermediate is stoichiometrically related to complex **2** and converts directly to the sulfenate complex **5**, thus eliminating the possibility of direct attack at sulfur. Whether the green intermediate is an oxo atom donor adduct, Fe-O=I-Ph, or an Fe(V)=O remains to be determined. Given how rare Fe-O=I-Ph[138,139] and Fe(V)=O[93,113,124] species are, both possibilities are intriguing. The λ_{max} of our green intermediate (677 nm) is in the reported range for both Fe(III)-O=I-Ph (λ_{max} = 660 nm)[139] and Fe(V)=O (λ_{max} = 630(5400 $M^{-1}cm^{-1}$) nm)[93,104] consistent with either possibility. Iodosylarene adducts have been shown to be competent oxidants in OAT reactions.[138-142] Spectroscopic characterization of the green intermediate, along with the kinetics of both its formation and conversion to sulfenate-ligated **5**, will be the topic of a separate manuscript. Possible mechanisms for sulfur oxygenation would involve initial formation of an oxo atom donor adduct Fe-O=I-

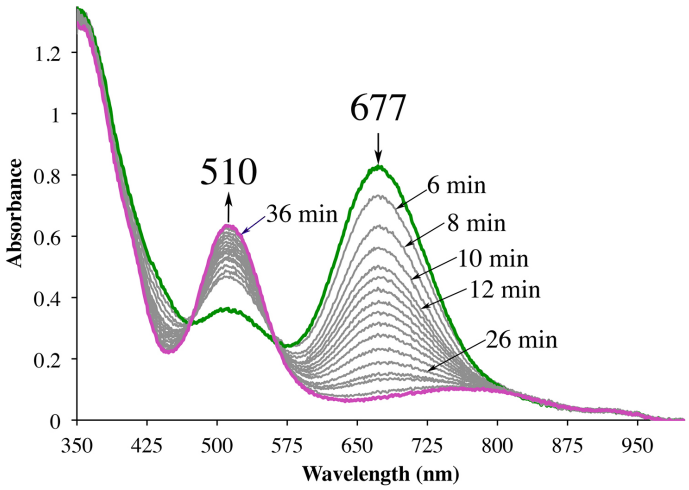

Figure 11. Detection of a green metastable intermediate in the reaction between (Pr,Pr)Fe(III) (**2**) and 10 eq. of IBX-ester at –73˚C in MeOH to form sulfenate **5** over the course of 36 minutes.

Ph that is either directly attacked by the adjacent nucleophilic sulfur, or which converts first to an Fe(V)=O, which is then rapidly and irreversibly trapped by the adjacent sulfur. The observation of one intermediate, as opposed to two, is consistent with either (a) rate-determining *cis*-migration of a thiolate sulfur to the oxo of a coordinated Fe-O=I-Ph, or (b) rate-determining cleavage of the I–O bond to afford an Fe(V)=O. The virtually identical electronic spectra associated with the green intermediate, regardless of the nature of the oxo atom donor is a bit puzzling, given that one would expect an Fe-O=I^{V}-Ph species to have electronic properties that differ from that of an Fe-O=I^{III}-Ph species. Inhibition studies, involving PhI, should help to distinguish mechanisms (a) and (b). The anticipated rapid rate of intramolecular trapping of an Fe(V)=O, relative to the likely rate of its formation, would suggest that it would be unobservable. This remains to be determined, however.

Summary and Conclusions. Cysteinate oxygenation is intimately tied to the function of both cysteinate dioxygenases (CDO)[1-8] and nitrile hydratases (NHases).[31,39-41] However, the mechanisms by which sulfurs are oxidized by these enzymes is unknown, in part because intermediates have yet to be observed. Herein we show that oxo atom donors, PhIO and H_2O_2, react with coordinatively unsaturated $[Fe^{III}(S_2{}^{Me2}N_3(Pr,Pr))]^+$ (**2**) to afford a rare example of a singly oxygenated sulfenate, $[Fe^{III}(\eta^2\text{-}S^{Me2}O)(S^{Me2})N_3(Pr,Pr)]^+$ (**5**). Sulfenate-ligated **5** is low-spin (S= ½; g= 2.17, 2.11, 1.98), and resembles both an intermediate proposed to form during CDO catalyzed cysteine oxidation, as well as the catalytically essential NHase Fe–S^{Cys114}–O, proposed to be intimately involved in its mechanism.[27,31,42,43] In contrast to imine-

ligated **2**, carboxamide-ligated $[Fe^{III}S_2{}^{Me2}N^{Me}N_2{}^{amide}(Pr,Pr)]^{1-}$ (**8**) was shown to be unreactive towards oxo atom donors PhIO or H_2O_2, under any conditions. DFT-calculated Mulliken charges on the sulfurs of anionic **8** were found to be roughly twice that of cationic **2**, indicating that if oxo atom donors were to directly attack the thiolate sulfur, then carboxamide-ligated **8** would be more reactive than imine-ligated **2**. Reactivity was shown to correlate with the metal ion's ability to bind exogenous ligands, and azide (N_3^-) was found to inhibit sulfur oxidation with **2**, suggesting that the mechanism of sulfur oxidation involves initial coordination of the oxo atom donor to the metal ion. Consistent with this, a green intermediate is observed to form, which then slowly converts to sulfenate-ligated **5**. Whether the green intermediate is an oxo atom donor adduct, Fe-O=I-Ph, or an Fe(V)=O remains to be determined. The placement of a nucleophilic thiolate *cis* to an electrophilic oxo would facilitate rapid intramolecular trapping of a high-valent oxo via the formation of an S-O bond. Although the direct involvement of the metal ion has been theoretically calculated to provide a lower energy pathway to sulfur oxygenation by CDO,[5] this has not been experimentally proven.[7]

Acknowledgements. This work was supported by NIH (GM45881). P. L. -M. gratefully acknowledges support by an NIH pre-doctoral minority fellowship (F31 GM73583-01). We also gratefully acknowledge Steven J. Lippard, and an anonymous donor for financial support.

Supporting Information. Contains experimental details regarding the synthesis and characterization of the [(Pr,Pr)($N^{Me}HN^{amide}{}_2{}^{Me}(SH)_2$)]•HCl ligand. ESI mass spec, IR, and cyclic voltammogram of **5**. ESI mass spec, IR, cyclic voltammogram, aqueous electronic absorption and EPR spectra of **8**, and electronic spectral evidence for the formation of **5**, via a green metastable intermediate. Crystallographic tables for **5** and **8,** and metrical parameters for DFT optimized structures are also included. This material is available free of charge via the Internet at http://pubs.acs.org.

References

(1) Kumar, D.; Sastry, G. N.; Goldberg, D. P.; de Visser, S. P. *J. Phys. Chem. A.* **2012**, *116*, 582-591.
(2) McQuilken, A. C.; Jiang, Y.; SIegler, M. A.; Goldberg, D. P. *J. Am. Chem. Soc.* **2012**, *134*, 8758-8761.
(3) Badiei, Y. M.; Siegler, M. A.; Goldberg, D. P. *J. Am. Chem. Soc.* **2011**, *133*, 1274-1277.
(4) Jiang, Y.; Widger, L. R.; Kasper, G. D.; Siegler, M. A.; Goldberg, D. P. *J. Am. Chem. Soc.* **2010**, *132*, 12214-12215.
(5) Kumar, D.; Thiel, W.; de Visser, S. P. *J. Am. Chem. Soc.* **2011**, *133*, 3869-3882.
(6) Aluri, S.; Visser, S. P. *J. Am. Chem. Soc* **2007**, *129*, 14846-14847.
(7) Simmons, C. R.; Krishnamoorthy, K.; Granett, S. L.; Schuller, D. J.; Dominy, J. E., Jr.; Begley, T. P.; Stipanuk, M. H.; Karplus, P. A. *Biochemistry* **2008**, *47*, 11390-11392.
(8) Ray, K.; Pfaff, F. F.; Wang, B.; Nam, W. *J. Am. Chem. Soc.* **2014**, *136*, 13942-13958.

(9) Heafield, M. T.; Fearn, S.; Steventon, G. B.; Waring, R. H.; Williams, A. C.; Sturman, S. G. *Neurosci. Lett.* **1990**, *110*, 216-220.
(10) Driggers, C. M., Stipanuk, M. H. and Karplus, P. A. *Mammalian Cysteine Dioxygenase*. In *Encyclopedia of Inorganic and Bioinorganic Chemistry* [Online]; John Wiley & Sons: New York, 2015; pp 1-11, http://onlinelibrary.wiley.com/doi/10.1002/9781119951438.eibc2326.
(11) Brait, M.; Ling, S.; Nagpal, J. K.; Chang, X.; Park, H. L.; Lee, J.; ; Okamura, J.; Yamashita, K.; Sidransky, D.; Kim, M. S. *PLOS One* **2012**, *7*, e44951.
(12) Jeschke, J.; O'Hagan, H. M.; Zhang, W.; Vatapalli, R.; Freitas Calmon, M.; ; Danilova, L.; Nelkenbrecher, C.; Van Neste, L.; Bijsmans, I. T. G. W.; ; Van Engeland, M.; Gabrielson, E.; Schuebel, K. E.; Winterpach, A.; Baylin, S. B.; ; Herman, J. G.; Ahuja, N. *Clin. Cancer Res.* **2013**, *19*, 3201-3211.
(13) Chiang, C.-W.; Kleepsies, S. T.; Stout, H. D.; Meier, K. K.; Li, P.-Y.; Bominaar, E. L.; Que, L., Jr.; Münck, E.; Lee, W.-Z. *J. Am. Chem. Soc.* **2014**, *136*, 10846-10849.
(14) Hong, S.; Sutherlin, K. D.; Park, J.; Kwon, E.; Siegler, M. A.; Solomon, E. I.; Nam, W. *Nature Comm.* [Online] **2014**, *5*, Article 6440. http://nature.com/articles/ncomms6440.
(15) Sahu, S.; Goldberg, D. P. *J. Am. Chem. Soc.* **2016**, *138*, 11410-11428.
(16) Mascharak, P. K.; Harrop, T. C. *Acc. Chem. Res.* **2004**, *37*, 253-260.
(17) Lugo-Mas, P.; Taylor, W.; Schweitzer, D.; Theisen, R. M.; Xu, L.; Shearer, J.; Swartz, R. D.; Gleaves, M. C.; DiPasquale, A.; Kaminsky, W.; Kovacs, J. A. *Inorg. Chem.* **2008**, *47*, 11228-11236.
(18) Noveron, J. C.; Olmstead, M. M.; Mascharak, P. K. *J. Am. Chem. Soc.* **2001**, *123*, 3247-3259.
(19) Tyler, L. A.; Noveron, J. C.; Olmstead, M. M.; Mascharak, P. K. *Inorg. Chem.* **2000**, *39*, 357-362.
(20) Heinrich, L.; Li, Y.; Vaissermann, J.; Chottard, G.; Chottard, J.-C. *Angew. Chem., Int. Ed.* **1999**, *38*, 3526-3528.
(21) Sallmann, M.; Siewert, I.; Fohlmeister, L.; Limberg, C.; Knispel, C. *Angew. Chem lnl. Ed.* **2012**, *51*, 2234-2237.
(22) McQuilken, A. C.; Goldberg, D. P. *Dalton Trans.* **2012**, *41*, 10883-10899.
(23) Widger, L. R.; Jiang, Y.; Siegler, M. A.; Kumar, D.; Latifi, R.; de Visser, S. P.; Jameson, G. N. L.; Goldberg, D. P. *Inorg. Chem.* **2013**, *52*, 10467-10480.
(24) Grapperhaus, C. A.; Darensbourg, M. Y. *Acc. Chem. Res.* **1998**, *31*, 451–459.
(25) Leonard, S. E.; Reddie, K. G.; Carroll, K. S. *ACS Chem. Biol.* **2009**, *4*, 783-799.
(26) Claiborne, A.; Yeh, J. I.; Mallet, C.; Luba, J.; Crane, E. J.; Charrier, V.; Parsonage, D. *Biochemistry* **1999**, *38*, 15407-15416.
(27) Light, K. M.; Yamanaka, Y.; Odaka, M.; Solomon, E. I. *Chem. Sci.* **2015**, *6*, 6280-6294.
(28) Hashimoto, K.; Suzuki, H.; Taniguchi, K.; Noguchi, T.; Yohda, M.; Odaka, M. *J. Biol. Chem.* **2008**, *283*, 36617-36623.
(29) Murakami, T.; Nojiri, M.; Nakayama, H.; Odaka, M.; Yohda, M.; Dohmae, N.; Takio, K.; Nagamune, T.; Endo, I. *Protein Sci.* **2000**, *9*, 1024-1030.
(30) Nojiri, M.; Yohda, M.; Odaka, M.; Matsushita, Y.; Tsujimura, M.; Yoshida, T.; Dohmae, N.; Takio, K.; Endo, I. *J. Biochem.* **1999**, *125*, 696-704.
(31) Martinez, S.; Wu, R.; Sanishvili, R.; Liu, D.; Holz, R. *J. Am. Chem. Soc.* **2014**, *136*, 1186-1189.
(32) Yeh, J. I.; Claiborne, A.; Hol, W. G. I. *Biochemistry* **1996**, *35*, 9951-9957.

(33) Chae, H. Z.; Robison, K.; Poole, L. B.; Church, G.; Storz, G.; Rhee, S. G. *Proc. Natl. Acad. Sci. U. S. A.* **1994**, *91*, 7017-7021.
(34) Mitra, S.; Holz, R. C. *J Biol Chem* **2007**, *282*, 7397-7404.
(35) Noguchi, T.; Nojiri, M.; Takei, K.; Odaka, M.; Kamiya, N. *Biochemistry* **2003**, *42*, 11642-11650.
(36) Kobayashi, M.; Shimizu, S. *Nat. Biotechnol.* **1998**, *16*, 733–736.
(37) Sugiura, Y.; Kuwahara, J.; Nagasawa, T.; Yamada, H. *J. Am. Chem. Soc.* **1987**, *109*, 5848-5850.
(38) Stolz, A.; Trott, S.; Binder, M.; Bauer, R.; Hirrlinger, B.; Layh, N.; Knackmuss, H.-J. *J. Mol. Catal. B: Enzym.* **1998**, *5*, 137-141.
(39) Dey, A.; Chow, M.; Taniguchi, K.; Lugo-Mas, P.; Davin, S. D.; Maeda, M.; Kovacs, J. A.; Odaka, M.; Hedman, B.; Hodgson, K. O.; Solomon, E. I. *J. Am. Chem. Soc.* **2006**, *128*, 533-541.
(40) Song, L.; Wang, M.; Shi, J.; Xue, Z.; Wang, M.-X.; Qian, S. *Biochem. Biophys. Res. Comm.* **2007**, *362*, 319-324.
(41) Nagashima, S.; Nakasako, M.; Naoshi, D.; Tsujimura, M.; Takio, K.; Odaka, M.; Yohda, M.; Kamiya, N.; Endo, I. *Nat. Struct. Biol.* **1998**, *5*, 347-351.
(42) Tsujimura, M. O., M.; Nakayama, H.; Dohmae, N.; Koshino, H.; Asami, T.; Hoshino, M.; Takio, K.; Yoshida, S.; Maeda, M.; Endo, I. *J. Am. Chem. Soc.* **2003**, *125*, 11532.
(43) Yamanaka, Y.; Kato, Y.; Hashimoto, K.; Iida, K.; Nagasawa , K.; Nakayama, H.; Dohmae, N.; Noguchi, K.; Noguchi, T.; Yohda, M.; Odaka, M. *Angew. Chem Int. Ed.* **2015**, *54*, 10763-10767.
(44) Goto, K.; Holler, M.; Okazaki, R. *J. Am. Chem. Soc.* **1997**, *119*, 1460-1461.
(45) Allison, W. S. *Acc. Chem. Res.* **1976**, *9*, 293–299.
(46) Adzamili, I. K.; Libson, K.; Lydon, J. D.; Elder, R. C.; Deutsch, E. *Inorg. Chem.* **1979**, *18*, 303–311.
(47) Bachi, M. D.; Gross, A. *J. Org. Chem.* **1982**, *47*, 897-898.
(48) Lugo-Mas, P.; Dey, A.; Xu, L.; Davin, S. D.; Benedict, J.; Kaminsky, W.; Hodgson, K. O.; Hedman, B.; Solomon, E. I.; Kovacs, J. A. *J. Am. Chem. Soc.* **2006**, *128*, 11211-11221.
(49) Kung, I. Y.; Schweitzer, D.; Shearer, J.; Taylor, W. D.; Jackson, H. L.; Lovell, S.; Kovacs, J. A. *J. Am. Chem. Soc.* **2000**, *122*, 8299-8300.
(50) Coggins, M. K. S., X.; Kwak, Y.; Solomon, E. I.; Rybak-Akimova, E. V.; Kovacs, J. A. *J. Am. Chem. Soc.* **2013**, *135*, 5631-5640.
(51) Theisen, R. M.; Shearer, J.; Kaminsky, W.; Kovacs, J. A. *Inorg. Chem.* **2004**, *43*, 7682–7690.
(52) Kovacs, J. A. *Science* **2003**, *299*, 1024-1025.
(53) Kitagawa, T.; Dey, A.; Lugo-Mas, P.; Benedict, J.; Kaminsky, W.; Solomon, E.; Kovacs, J. A. *J. Am. Chem. Soc.* **2006**, *128*, 14448-14449.
(54) Shearer, J.; Scarrow, R. C.; Kovacs, J. A. *J. Am. Chem. Soc.* **2002**, *124*, 11709-11717.
(55) Kovacs, J. A. *Acc. Chem. Res.* **2015**, *48*, 2744-2753.
(56) Coggins, M. K.; Martin-Diaconescu, V.; De Beer, S.; Kovacs, J. A. *J. Am. Chem. Soc.* **2013**, *135*, 4260-4272.
(57) Coggins, M. K.; Brines, L. M.; Kovacs, J. A. *Inorg. Chem.* **2013**, *52*, 12383-12393.
(58) Coggins, M. K.; Kovacs, J. A. *J. Am. Chem. Soc* **2011**, *133*, 12470-12473.
(59) Kovacs, J. A.; Brines, L. M. *Acc. Chem. Res.* **2007**, *40*, 501-509.
(60) Kovacs, J. A. *Chem. Rev.* **2004**, *104*, 825-848.

(61) Schweitzer, D.; Shearer, J.; Rittenberg, D. K.; Shoner, S. C.; Ellison, J. J.; Loloee, R.; Lovell, S. C.; Barnhart, D. K., J. A. *Inorg. Chem.* **2002**, *41*, 3128-3136.
(62) Shoner, S. C.; Nienstedt, A.; Ellison, J. J.; Kung, I.; Barnhart, D.; Kovacs, J. A. *Inorg. Chem.* **1998**, *37*, 5721-5725.
(63) Ellison, J. J.; Nienstedt, A.; Shoner, S. C.; Barnhart, D.; Cowen, J. A., Kovacs, J. A. *J. Am. Chem. Soc.* **1998**, *120*, 5691-5700.
(64) Shearer, J.; Nehring, J.; Kaminsky, W.; Kovacs, J. A. *Inorg. Chem.* **2001**, *40*, 5483-5484.
(65) Shearer, J.; Fitch, S. B.; Kaminsky, W.; Benedict, J.; Scarrow, R. C.; Kovacs, J. A. *Proc. Natl. Acad. Sci., USA* **2003**, *100*, 3671-3676.
(66) Shearer, J.; Jackson, H. L.; Schweitzer, D.; Rittenberg, D. K.; Leavy, T. M.; Kaminsky, W.; Scarrow, R. C.; Kovacs, J. A. *J. Am. Chem. Soc.* **2002**, *124*, 11417–11428.
(67) Theisen, R.; Shearer, J.; Kaminsky, W.; Kovacs, J. *Inorg Chem* **2004**, *43*, 7682-7690.
(68) Grapperhaus, C. A.; Li, M.; Patra, A. K.; Poturovic, S.; Kozlowski, P. M.; Zgierski, M. Z.; Mashuta, M. S. *Inorg. Chem.* **2003**, *42*, 4382-4388.
(69) Namuswe, F.; Kasper, G. D.; Narducci Sarjeant, A. A.; Hayashi, T.; Krest, C. M.; Green, M. T.; Moenne-Loccoz, P.; Goldberg, D. P. *J. Am. Chem. Soc.* **2008**, *130*, 14189-14200.
(70) Jiang, Y.; Telser, J.; Goldberg, D. P. *Chem. Comm.* **2009**, 6828-6830.
(71) Shearer, J.; Nehring, J.; Lovell, S.; Kaminsky, W.; Kovacs, J. *Inorg Chem* **2001**, *40*, 5483-5484.
(72) Brines, L. M.; Shearer, J.; Fender, J. K.; Schweitzer, D.; Shoner, S. C.; Barnhart, D.; Kaminsky, W.; Lovell, S.; Kovacs, J. A. *Inorg. Chem.* **2007**, *46*, 9267-9277.
(73) Brines, L. M.; Villar-Acevedo, G.; Kitagawa, T.; Swartz, R. D.; Lugo-Mas, P.; Kaminsky, W.; Benedict, J. B.; Kovacs, J. A. *Inorg Chim Acta* **2008**, *361*, 1070-1078.
(74) Shearer, J.; Kung, I., Lovell, S. Kovacs, J. A. *Inorg. Chem.* **2000**, *39*, 4998–4999.
(75) Theisen, R. M.; Kovacs, J. A. *Inorg. Chem.* **2005**, *44*, 1169-1171.
(76) Villar-Acevedo, G.; Nam, E.; Fitch, S.; Benedict, J.; Freudenthal, J.; Kaminsky, W.; Kovacs, J. A. *J. Am. Chem. Soc.* **2011**, *133*, 1419-1427.
(77) Nam, E.; Alokolaro, P. E.; Swartz, R. D.; Gleaves, M. C.; Pikul, J.; Kovacs, J. A. *Inorg. Chem.* **2011**, *50*, 1592-1602.
(78) Schweitzer, D.; Ellison, J. J.; Shoner, S. C.; Lovell, S.; Kovacs, J. A. *J. Am. Chem. Soc.* **1998**, *120*, 10996-10997.
(79) Kennepohl, P.; Neese, F.; Schweitzer, D.; Jackson, H. L.; Kovacs, J. A.; Solomon, E. I. *Inorg. Chem.* **2005**, *44*, 1826-1836.
(80) Shearer, J.; Kung, I. Y.; Lovell, S.; Kaminsky, W.; Kovacs, J. A. *J. Am. Chem. Soc.* **2001**, *123*, 463-468.
(81) Live, D. H.; Chan, S. I. *Anal. Chem.* **1970**, *42*, 791.
(82) Evans, D. A. *J. Chem. Soc.* **1959**, 2005.
(83) Van Geet, A. L. *Anal. Chem.* **1968**, *40*, 2227-2229.
(84) Neese, F. *Interdiscip. Rev. Comput. Mol. Sci.* **2012**, *2*, 73-78.
(85) Becke, A. D. *Phys. Rev. A: Gen. Phys.* **1988**, *38*, 3098-3100.
(86) Perdew, J. P. *Phys. Rev. B* **1986**, *33*, 8822-8224.
(87) Weigend, F. *Phys. Chem. Chem. Phys.* **2006**, *8*, 1057-1065.
(88) Grimme, S.; Ehrlich, S.; Goerigk, L. *J. Comput. Chem* **2011**, *32*, 1456-1465.
(89) Lenthe, E. V.; Avoird, A. V. D.; Wormer, P. E. S. *J. Chem. Phys.* **1998**, *109*, 392-399.
(90) Weigend, F.; Ahlrichs, R. *Phys. Chem. Chem. Phys.* **2005**, *7*, 3297-3305.
(91) Klamt, A.; Schüürmann, G. *J. Chem. Soc., Perkin Trans.* **1993**, *5*, 799-805.

(92) Waasmaier, D.; Kirfel, A. *Acta Crystallogr. A.* **1995**, *51*, 416.
(93) de Oliveira, F. T.; Chanda, A.; Banerjee, D.; Shan, X.; Mondal, S.; Que, L., Jr.; Bominaar, E. L.; Münck, E.; Collins, T. J. *Science* **2007**, *315*, 835-838.
(94) Lyakin, O. Y.; Zima, A. M.; Samsonenko, D. G.; Bryliakov, K. P.; Talsi, E. P. *ACS Catal.* **2015**, *5*, 2702-2707.
(95) Ghosh, M.; Singh, K. K.; Panda, C.; Weitz, A.; Hendrich, M. P.; Collins, T. J.; Dhar, B. B.; Gupta, S. S. *J. Am. Chem. Soc.* **2014**, *136*, 9524-9527.
(96) Van Heuvelen, K. M.; Fiedler, A. T.; Shan, X.; De Hont, R. F.; Meier, K. K.; Bominaar, E. L.; Münck, E.; Que, L., Jr. *Proc. Natl. Acad. Sci, USA* **2012**, *109*, 11933-11938.
(97) Jackson, H. L.; Shoner, S. C.; Rittenberg, D.; Cowen, J. A.; Lovell, S.; Barnhart, D.; Kovacs, J. A. *Inorg. Chem.* **2001**, *40*, 1646-1653.
(98) Que, L., Jr. *Acc. Chem. Res.* **2007**, *40*, 493-500.
(99) Rohde, J.-U.; In, J. H.; Lim, M. H.; Brennessel, W. W.; Bukowski, M. R.; Stubna, A.; Münck, E.; Nam, W.; Que, L., Jr. *Science* **2003**, *299*, 1037-1039.
(100) Sastri, C. V.; Park, M. J.; Ohta, T.; Jackson, T. A.; Stubna, A.; Seo, M. S.; Lee, J.; Kim, J.; Kitagawa, T.; Münck, E.; Que, L., Jr.; Nam, W. *J. Am. Chem. Soc.* **2005**, *127*, 12494-12495.
(101) Nam, W.; Jin, S. W.; Lim, M. H.; Ryu, J. Y. *Inorg. Chem.* **2002**, *41*, 3647-3652.
(102) Nam, W.; Choi, S. K.; Lim, M. H.; Rohde, J.-U.; Kim, I.; Kim, J.; Kim, C.; Que, L., Jr. *Angew. Chem lnl. Ed.* **2003**, *42*, 109-111.
(103) Groves, J. T.; Watanabe, Y. *J. Am. Chem. Soc.* **1988**, *110*, 8443-8452.
(104) Kundu, S.; Van Kirk Thompson, J.; Ryabov, A. D.; Collins, T. J. *J. Am. Chem. Soc.* **2011**, *133*, 18546-18549.
(105) Meunier, B.; de Visser, S. P.; Shaik, S. *Chem. Rev.* **2004**, *104*, 3947-3980.
(106) Rittle, J.; Green, M. T. *Science* **2010**, *330*, 933-937.
(107) Krest, C. M.; Onderko, E. L.; Yosco, T. H.; Calixto, J. C.; Karp, R. F.; Livada, J.; Rittle, J.; Green, M. T. *J. Biol. Chem.* **2013**, *288*, 17074-17081.
(108) Wang, X.; Peter, S.; Kinne, M.; Hofrichter, M.; Groves, J. T. *J. Am. Chem. Soc.* **2012**, *134*, 12897-12900.
(109) Chreifi, G.; Baxter, E. L.; Doukov, T.; Cohen, A. E.; McPhillips, S. E.; Song, J.; Meharenna, Y. T.; Soltis, S. M.; Poulos, T. L. *Proc. Natl. Acad. Sci, USA* **2016**, *113*, 1226-1231.
(110) Barrows, T. P.; Poulos, T. L. *Biochemistry* **2005**, *44*, 14062-14068.
(111) Denisov, I. G.; Makris, T. M.; Sligar, S. G.; Schlichting, I. *Chem. Rev.* **2005**, *105*, 2253-2277.
(112) Oloo, W. N.; Que, L., Jr. *Acc. Chem. Res.* **2015**, *48*, 2612-2621.
(113) Prat, E.; Mathieson, J. S.; Guell, M.; Ribas, X.; Luis, J. M.; Cronin, L.; Costas, M. *Nature Chem.* **2011**, *3*, 788-793.
(114) Decker, A.; Rohde, J.-U.; Klinker, R. J.; Wong, S. D.; Que, L. J.; Solomon, E. I. *J. Am. Chem. Soc.* **2007**, *129*, 15983-15996.
(115) Bukowski, M. R.; Koehntop, K. D.; Stubna, A.; Bominaar, E. L.; Halfen, J. A.; Münck, E.; Nam, W.; Que, L. *Science* **2005**, *310*, 1000-1002.
(116) Costas, M.; Mehn, M. P.; Jensen, M. P.; Que, L. J. *Chem. Rev.* **2004**, *104*, 939-986.
(117) Puri, M.; Que, L., Jr. *Acc. Chem. Res.* **2015**, *48*, 2443-2452.

(118) Sahu, S.; Quesne, M. G.; Davies, C. G.; Dürr, M.; Ivanovic´-Burmazovic, I.; Siegler, M. A.; Jameson, G. N. L.; de Visser, S. P.; Goldberg, D. P. *J. Am. Chem. Soc.* **2014**, *136*, 13542-13545.
(119) Lacy, D. C.; Gupta, R.; Stone, K. L.; Greaves, J.; Ziller, J. W.; Hendrich, M. P.; Borovik, A. S. *J. Am. Chem. Soc.* **2010**, *132*, 12188-12190.
(120) Solomon, E. I.; Wong, S. D.; Liu, L. V.; Decker, A.; Chow, M. S. *Curr. Op. Chem. Biol.* **2009**, *13*, 99-113.
(121) Nam, W. *Acc. Chem. Res.* **2015**, *48*, 2415-2423.
(122) Thibon, A.; England, J.; Martinho, M.; Young, V. G., Jr.; Frisch, J. R.; Guillot, R.; Girerd, J.-J.; Münck, E.; Que, L., Jr.; Banse, F. *Angew. Chem lnl. Ed.* **2008**, *47*, 7064-7067.
(123) Hohenberger, J.; Ray, K.; Meyer, K. *Nature Comm.* **2012**, *3*, 1-13.
(124) McDonald, A. R.; Que, L., Jr. *Nature Chem.* **2011**, *3*, 761-762.
(125) Kundu, S.; Thompson, J. V. K.; Shen, L. Q.; Mills, M. R.; Bominaar, E. L.; Ryabov, A. D.; Collins, T. J. *Chem. Eur. J.* **2015**, *21*, 1803-1810.
(126) Panda, C.; Debgupta, J.; Díaz, D. D.; Singh, K. K.; Gupta, S. S.; Dhar, B. B. *J. Am. Chem. Soc.* **2014**, *136*, 12273-12282.
(127) Groves, J. T.; Haushalter, R. C.; Nakamura, M.; Nemo, T. E.; Evans, B. J. *J. Am. Chem. Soc.* **1981**, *103*, 2884-2886.
(128) Buonomo, R. M.; Font, I.; Maguire, M. J.; Reibenspies, J. H.; Tuntulani, T.; Darensbourg, M. Y. *J. Am. Chem. Soc.* **1995**, *117*, 963-973.
(129) Heinrich, L.; Mary–Verla, A.; Li, Y.; Vaissermann, J.; Chottard, J. C. *Eur. J. Inorg. Chem.* **2001**, 2203-2206.
(130) Lydon, J. D.; Deutsch, E. *Inorg. Chem.* **1982**, *21*, 3180–3185.
(131) Cornman, C. R.; Stautler, T. C.; Boyle, P. D. *J. Am. Chem. Soc.* **1997**, *119*, 5986-5987.
(132) Ge, W.; Clifton, I. J.; Stok, J. E.; Adlington, R. M.; Baldwin, J. E.; Rutledge, P. J. *J. Am. Chem. Soc.* **2008**, *130*, 10096-10102.
(133) Noveron, J. C.; Olmstead, M. M.; Mascharak, P. K. *Inorg. Chem.* **1998**, *37*, 1138–1139.
(134) Costas, M.; Harvey, J. N. *Nature Chem.* **2013**, *5*, 7-9.
(135) Carreon-Macedo, J.-L.; Harvey, J. N. *J. Am. Chem. Soc.* **2004**, *126*, 5789-5797.
(136) Shoner, S.; Barnhart, D.; Kovacs, J. A. *Inorg. Chem.* **1995**, *34*, 4517-4518.
(137) Ye, W.; Ho, D. M.; Friedle, S.; Palluccio, T. D.; Rybak-Akimova, E. V. *Inorg. Chem.* **2012**, *51*, 5006-5021.
(138) Lennartson, A.; McKenzie, C. J. *Angew. Chem lnt. Ed.* **2012**, *51*, 6767-6770.
(139) Hong, S.; Wang, B.; Seo, M. S.; Lee, Y. M.; Kim, M. J.; Kim, H. R.; Ogura, T.; Garcia-Serres, R.; Clémancey, M.; Latour, J. M.; Nam, W. *Angew. Chemie Int. Ed.* **2014**, *53*, 6388-6392.
(140) Wang, C.; Kurahashi, T.; Inomata, K.; Hada, M.; Fujii, H. *Inorg. Chem.* **2013**, *52*, 9557-9566.
(141) Wang, S. H.; Mandimutsira, B. S.; Todd, R.; Ramdhanie, B.; Fox, J. P.; Goldberg, D. P. *J. Am. Chem. Soc.* **2004**, *126*, 18-19.
(142) Yang, Y.; Diederich, F.; Valentine, J. S. *J. Am. Chem. Soc.* **1990**, *112*, 7826-7828.

TOC Graphic

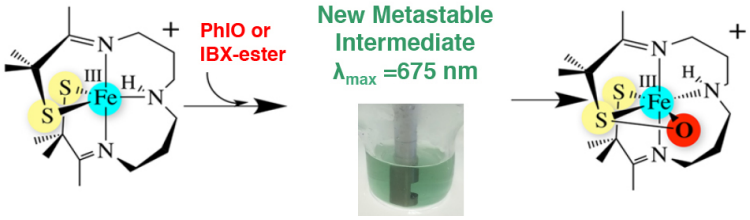
PhIO or
IBX-ester
New Metastable
Intermediate
λmax =675 nm